# COMMISSIONING AND EARLY OPERATION OF THE ARIEL E-LINAC*

T. Planche†, M. Marchetto‡, M.M. Alcorta, F.A. Ames, R.A. Baartman, C.B. Barquest,
B. Humphries, D. Kaltchev, S.R. Koscielniak, R.E. Laxdal, Y. Ma,
E. Thoeng, S. Saminathan, TRIUMF, Vancouver, Canada
P.M. Jung, University of Waterloo, Canada

*Abstract*

The ARIEL electron linac has been added to the TRIUMF facility as a new driver for the production of radioactive isotopes through photo-fission to complement the existing 500 MeV, $H^-$ TRIUMF cyclotron. The electron beam driver is specified as a 50 MeV, 10 mA cw superconducting electron linac at 1.3 GHz. The first 30 MeV stage of the e-linac consisting of two cryomodules is completed. The paper will describe the recent commissioning and early operation results.

## INTRODUCTION

The ARIEL facility [1, 2] is expected to triple the availability of radioactive beams at TRIUMF. This facility complements the existing ISAC facility, adding to it two driver beams: an additional proton beam from the existing 500 MeV $H^-$ TRIUMF cyclotron, and an electron beam from our new electron linac. The electron linac (e-linac) is designed to produce a 50 MeV, 10 mA cw beam using five 1.3 GHz nine-cell superconducting rf cavities distributed in three different cryomodules. In the present stage, only two cryomodules have been installed, limiting the achievable energy to around 30 MeV.

In this paper we report the progress made with machine commissioning since September 2014, when the first high-energy (22.9 MeV) low-power electron beam was demonstrated [2]. We have since put our beam dynamics models to the test; we now have available an accurate lightweight optics model of our entire linac (which includes 3-dimensional space-charge). We have encountered a variety of issues, ranging from beam optics to machine and personnel safety, that have been studied and addressed. Peak and average beam power are gradually being brought up; 1 kW of average beam power has recently been delivered to our very first users: our own target and ion-source development group.

## TESTING OUR MODELS

### *Optics model*

Different codes are used at TRIUMF to study different aspects of the electron beam dynamics: `GPT` for gun simulations, `ASTRA` from non-linear dynamics with space-charge, `G4beamline` for collimation studies, `COSY-∞` for non-linear optics, etc. But our main workhorse is the envelope code `TRANSOPTR` [3]. Rather than tracking a large number of macro-particles, this code keeps track of statistical quantities of the beam distribution: its 21 independent second moments. This is achieved by numerically integrating the envelope equation (in contrast with matrix codes like `TRANSPORT`); it includes 3-dimensional linear space-charge.

The gain in computation time compared to multi-particle space-charge codes is such that multi-parameter optimizations through our entire linac converge within seconds [4].

The code also estimates 2nd and 3rd order aberrations from dipoles, quadrupoles and solenoids. This allows the user to make sure that the simulation stays within the bounds of the model, i.e. linear optics. It can also be used to constrain the optimizer to converge to tunes with minimal non-linear aberration.

A comparison between the calculated envelope and measured beam size for a 9 MeV tune through the first accelerating cryomodule is shown in Fig. 1.

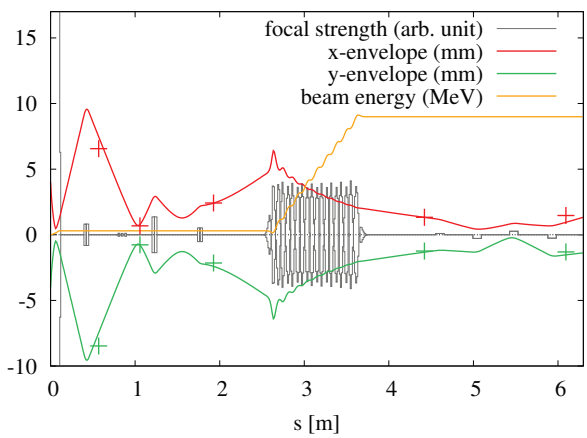


Figure 1: **Solid lines** present results of a `TRANSOPTR` simulation, which starts near rest on the e-gun grid, and goes through the injector cryomodule; **Crosses** present actual 2*rms beam size measured on view screens. The beam-energy curve (yellow) rises from 300 keV to 9 MeV; the 9-cell structure of the superconducting rf cavity is reflected in this curve.

A web-based graphical user interface (GUI) has been developed for this code (see Fig. 2). The choice of a browser based interface makes this tool reliable and platform-independent [5]. This GUI greatly facilitated commissioning, and is now used daily by operators.

* ARIEL is funded by the Canada Foundation for Innovation, the Provinces AB, BC, MA, ON, QC, and TRIUMF. TRIUMF receives funding via a contribution agreement with the National Research Council of Canada.
† tplanche@triumf.ca
‡ marco@triumf.ca

Figure 2: Screen capture of TRANSOPTR web-GUI (URL: http://hlaweb.triumf.ca/beam/envelope/). The simulation starts near rest on the e-gun grid, and goes through two accelerating cryomodules. The turnaround time for an individual calculation is so rapid (25 ms) that the envelopes are seen to change continuously as the sliders (in the top grey box) are moved. The check boxes on the right of the slider flag those elements that are adjusted by the optimizer routines. Optimization objectives are built into the beamline's description.

### *Initial Beam Properties*

The source of electrons is a 300 keV rf modulated thermionic electron gun (e-gun) [6]. The accuracy of our simulations depends on accurate input beam properties. Initial transverse beam parameters have been fitted from measured beam profiles. In the TRANSOPTR code, given an initial

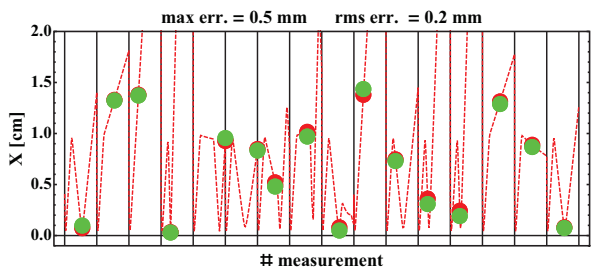


Figure 3: **Green dots:** measured beam sizes at three 300 keV view screens (for 16 solenoid settings) used to fit initial beam parameters at cathode. **Dashed red:** the 16 envelopes resulting from propagation of the resultant fitted initial beam. **Red dots:** propagated envelope values at the view screens.

beam represented by its phase space projections, assumed to be uncoupled, the sigma matrix (beam envelopes) computed with space charge is propagated along the beam-line. Also initial-beam ellipses and emittances can be fitted in a least-square sense, which is achieved by adding a loop over $N$ measurements, each corresponding to some focusing setup and producing corresponding $x$-$y$ beam sizes at an intermediate location (view screen). Such fits were performed at the e-gun grid, a fraction of a millimeter downstream of the cathode. The gun region is modeled using a calculated on-axis electric potential map. Satisfyingly, the fitted initial 2*rms beam size matched the known cathode radius (4 mm).

Figure 3 presents results from such a fit at cathode based on $N = 16$ measurements performed over a time span of three days and for bunch charges ranging from $1.6\times10^{-13}$ to $5.3\times10^{-12}$ C. On this figure the measured beam sizes (green) are seen to agree with predicted by TRANSOPTR values (red) to within a fraction of a millimeter. The normalized rms transverse emittance value found was 3.5 µm, which is in good agreement with previous measurements [2].

Another important parameter, for space-charge calculation, is the initial bunch length. The bunch length is measured at 300 keV, for various gun parameters, by looking at beam profiles downstream of a 650 MHz rf deflector, see Figs. 4 and 5. It is found to vary little with bunch charge, and depend mostly on the DC bias of the rf gun grid.

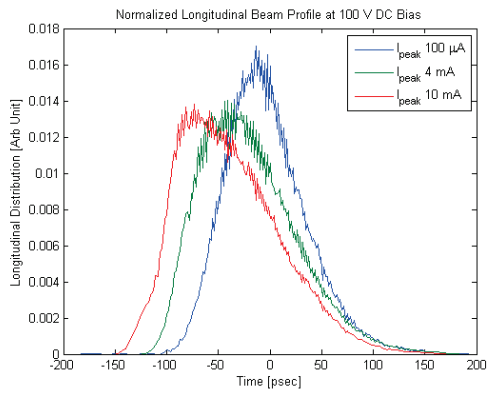


Figure 4: Longitudinal beam profiles for different bunch charges measured by means of a 650 MHz rf deflector.

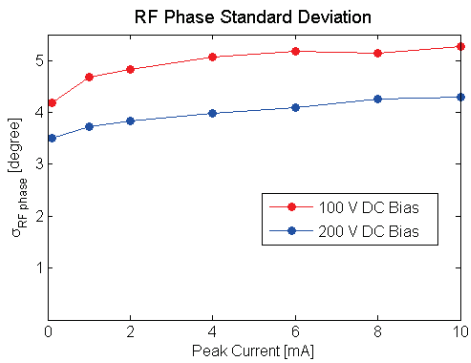


Figure 5: RMS bunch length, here expressed in degrees of 650 MHz rf phase, for various e-gun parameters; calculated from measurements similar to those presented in Fig. 4.

## TOWARD RELIABLE OPERATION

### *Ambient Field Compensation*

The entire electron linac is immersed in a stray magnetic field of several Gauss in magnitude. The two main sources of stray field are: (1) the 500 MeV cyclotron in the adjacent vault; (2) the remanent magnetization of the structural steel in the floor under the linac. Helmholtz coils are used to compensate the field contribution from the cyclotron. The




ISBN 978-3-95450-169-4

floor of the e-linac vault has been permanently demagnetized. For more detail see Ref. [7]. The remaining ambient field (no larger than the earth's magnetic field) is well within the range of our steering correctors.

### *Reproducibility of Steering Correctors*

A lesson learned from our low energy test stand [8] is that reproducible steering correctors is essential to simplify commissioning and achieve reliable operations. For the beam position to be reproducible to within a fraction its size, the field integral from each steering corrector must be reproducible to better than:

- 0.5 G.cm in the low-energy section (300 keV);
- 5 G.cm in the medium-energy (10 MeV) and high-energy (30-50 MeV) sections.

Requirement for the low energy section could not be achieved with steel-core steerers due to magnetic hysteresis. Air-core steerers with printed circuit coils, purchased from Radiabeam (and modified in house to accommodate engineering constraints) are used instead. Reproducibility of the beam position is excellent, leading to minimal tuning time.

At higher energies, stronger steel-core steerers are required. A first set of steerer purchased 'off-the-shelf' from Radiabeam showed too much hysteresis and were discarded (see Fig. 6). The second set of custom-made steerers proved to be about ~3 times better, but still exceeding our initial requirement by a factor ~4 (see Fig. 6). Those steerers have been installed.

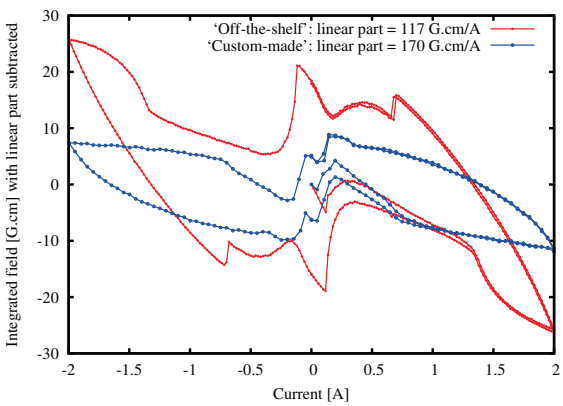


Figure 6: Results of magnetic measurement performed in house on two types of Radiabeam steel-core steerer; it shows the hysteresis curve with linear part subtracted. Hysteresis causes a non-reproducibility of 50 G.cm with the 'off-the-shelf' type. The origin of the complicated shape of this hysteresis curve, with sudden jumps bellow 1 A, remains uncertain; it seems to indicate a composite structure of the yoke, with a possible role played by the outside nickel-like coating of the steel parts. The reproducibility of the custom-made steerers is almost 3 times better.

### *Solenoid Repair*

The electron gun solenoid is the first optical downstream of the e-gun; it is embedded inside the gun high-voltage $SF_6$ vessel. To satisfy both engineering constraints and beam optics requirements, this solenoid is equipped with detachable magnetic field clamps. In its initial configuration these field clamps were mounted directly onto the vacuum chamber (see Fig. 8).

The first beam tests revealed: that the beam was exiting the e-gun solenoid with an unexpectedly large angle; that this angle was not reproducible; and that the beam did not show the expected cylindrical symmetry.

Magnetic measurements carried out *in situ* (see Fig. 7) showed an azimuthal variation of the magnetic filed (see plot in Fig. 8). Disassembling the solenoid revealed that the bottom half of the upstream field clamp had become loose and was poorly aligned (see picture in Fig. 8); 3-D magnetic calculation confirmed that this could cause the measured field asymmetry.

The two field clamps were re-designed: they are now dowel-pinned into the solenoid yoke. A new set of magnetic measurements confirmed that cylindrical symmetry of the field is recovered (see Fig. 9).

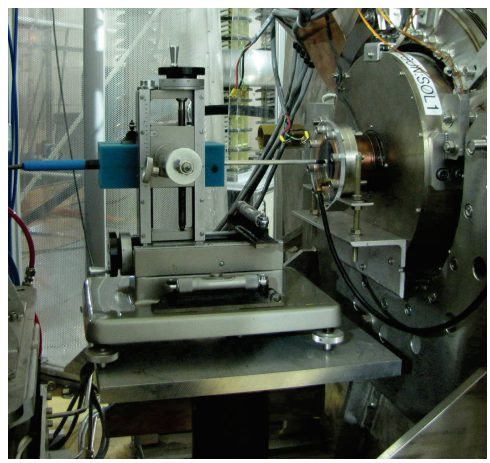

Figure 7: *In situ* magnetic measurement set-up: the cylinder on the right labelled "EGUN:SOL1" is the e-gun solenoid; the 3-axis Hall probe is mounted onto a rudimentary 3-axis table; the probe holder was precisely machined, and aligned with a precision better than 0.1 mm using a laser tracker.

Since the replacement of the field clamps the electron beam regained its cylindrical symmetry (see Fig. 10). Steering from the e-gun solenoid has become negligible: the strong (steel-core) steering corrector that had been installed immediately downstream of the solenoid is not used anymore. This greatly improves the reproducibility of our tunes and simplified the tuning procedure.

### *Upgrade of Safety Procedures*

Some considerable delay in the e-linac beam commissioning resulted from a safety incident that initiated a review of our internal protocols. Since it may be illustrative to other

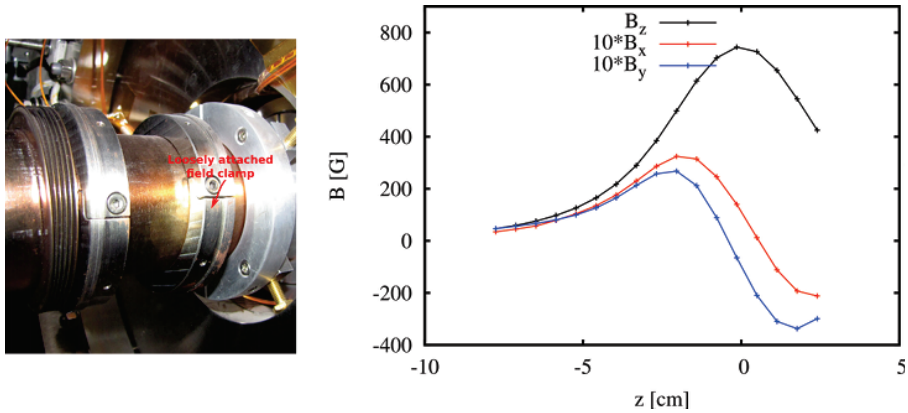


Figure 8: E-gun solenoid field clamp in its original configuration: attached to the beam pipe. This configuration resulted in loosely attached and poorly aligned field clamps (pictured on the left); magnetic field measured in-situ (plot on the right), parallel to the solenoid axis (and a few millimeters off-axis), revealed a strong violation of the cylindrical symmetry.

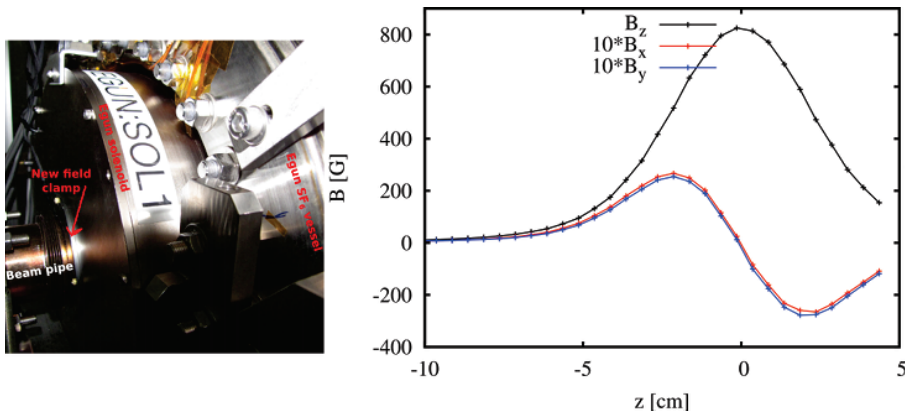


Figure 9: E-gun solenoid field clamp in its current configuration: mechanically attached to the solenoid yoke. Measurements (plot on the right) confirmed that the cylindrical symmetry of the magnetic field is restored.

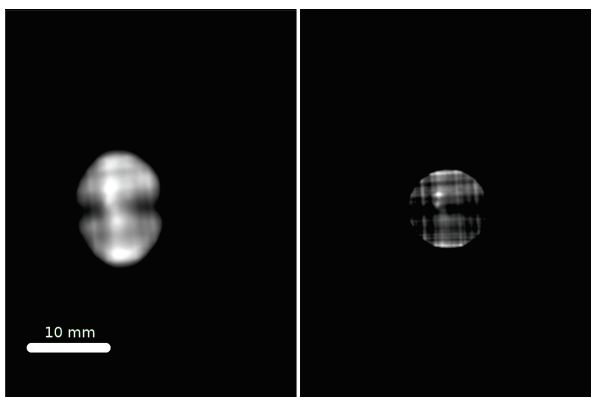


Figure 10: Beam image on the first view screen downstream of the e-gun, taken with the same setting of the e-gun solenoid (3.15 A), before (left) and after (right) the replacement of the field clamps. (The grid structure seen on the right appears because the phase advance between the gun grid and this view screen is close to 180 degrees.)

projects we summarize the incident here. The initial phase of commissioning took place while installation of major components was still on going. Installation was scheduled during the day with lock-up and commissioning in the evening. In September 2014 a person was missed during a lock-up search; this person safely exited the vault at the sound of the lock-up alarm but a decision was made to pause commissioning until our safety procedures and commissioning documents were thoroughly reviewed. Corrective actions included:

- a decision to avoid alternating installation with commissioning on a daily basis in favour of planning blocks of installation followed by blocks of commissioning on a weekly schedule;
- installation of more watch-man stations in order to guarantee a more thorough lock-up search;
- a review and improvement of the training of all personnel involved with installation and commissioning – in particular a directive that the personnel conducting the lock-up would be independent of the commissioning team.

During this period the training of all TRIUMF staff was reviewed and updated. Beam commissioning restarted in November 2015.




ISBN 978-3-95450-169-4

## TOWARD HIGHER BEAM POWER

### *Machine Protection System Commissioning*

The main objective of the machine protection system is to protect the beamline components against damages caused by accidental or chronic beam loss. The specification of such a system depends on processes happening on two different time scales [9].

The shorter time scale is related to the rate of heat deposition from the beam. Neglecting heat diffusion, the time it takes for matter to reach its melting temperature $T_m$ is given by:

$$\Delta t = \frac{2\pi\sigma_x\sigma_y C_p T_m}{\rho S(E) I/e}, \quad (1)$$

where $\rho$ is the material density, $S(E)$ the stopping power, $I$ the beam current, $e$ the electron charge, $\sigma_x$ and $\sigma_y$ the rms sizes of the beam distribution (along major/minor axises), and $C_p$ the heat capacity of the exposed material; $\Delta t$ is typically of the order of a fraction of a millisecond for our linac [9]. This time scale sets how rapidly our machine protection system must respond to catastrophic beam losses and stop the beam.

The longer time scale is related to the heat diffusion time constant. The diffusion equation is:

$$\frac{\partial T}{\partial t} = \alpha\, \nabla^2 T\,. \quad (2)$$

The time $\tau$ it takes for the heat to diffuse away is approximately given by:

$$\frac{1}{\tau} = \alpha\left(\frac{1}{\sigma_x^2} + \frac{1}{\sigma_y^2}\right), \quad (3)$$

Below this time scale, heat does not have time to diffuse away; $\tau$ is typically of the order of a few millisecond for our linac [9]. This time scale sets the time over which our machine protection system must integrate beam losses.

Our machine protection system relies on radiation monitors (photo-multiplier tubes) installed along the beam line. We are currently in the process of calibrating the output of these monitors using localized controlled beam losses.

### *Target Test Stand Facility*

To test the technologies required for our future high-power photo-fission convertor/target, a target test facility has been installed at the end of our 300 keV dump line. Average beam power of up to 1 kW has been delivered onto test targets; rms beam size can be made as small as ~1 mm, reproducing power density levels expected onto future high-energy convertor. Experimental study of various possible convertor materials (see Fig. 11) is on-going.

Figure 11: Example of two test targets; left: explosion bonded gold on aluminum; right: electro-plated gold on aluminum.

## CONCLUSION

Our beam optics model has been successfully tested. Operation of our 30 MeV electron linac has been made reliable and safe. 1 kW DC beam has successfully been delivered to our 300 keV target test facility. We are now aiming at gradually increasing the beam power going into and out of our superconducting rf cavities.

## REFERENCES

[1] L. Merminga, F. Ames, R. Baartman, P. Bricault, Y. Bylinski, Y. Chao, R. Dawson, D. Kaltchev, S. Koscielniak, R. Laxdal *et al.*, "ARIEL: TRIUMF's advanced rare isotope laboratory", in *Proc. of IPAC'11*, San Sebastián, Spain, paper WEOBA01, 2011.

[2] M. Marchetto, F. Ames, Z. Ang, R. Baartman, I. Bylinskii, Y. Chao, D. Dale, K. Fong, R. Iranmanesh, F. Jones, *et al.*, "Commissioning and operation of the ARIEL electron linac at TRIUMF", in *Proc. IPAC'15*, Richmond, VA, USA, paper WEYC3, 2015.

[3] M. S. de Jong and E. A. Heighway, "A first order space charge option for transoptr", *IEEE Transactions on Nuclear Science*, vol. 30, no. 4, pp. 2666–2668, Aug 1983.

[4] R. Baartman, "Fast Envelope Tracking for Space Charge Dominated Injectors", presented at LINAC'16, East Lansing, MI, USA, paper FR1A01, this conference.

[5] P. Jung, "Web applications for accelerator physics facilities", TRIUMF, Tech. Rep. TRI-BN-15-13, 2015.

[6] F. Ames, "The TRIUMF ARIEL rf Modulated Thermionic Electron Source", presented at LINAC'16, East Lansing, MI, USA, paper TUPRC020, this conference.

[7] T. Planche, G. Arias, R. Baartman, D. Bissky Dziadyk, S. Koscielniak, T. LeRoss, K. Multani, and T. Zuiderveen, "Demagnetization of an entire accelerator vault", in *Proc. IPAC'16*, Busan, Korea, May 2016, DOI: https://doi.org/10.18429/JACoW-IPAC2016-THPOY024.

[8] V. Naik *et al.*, "VECC/TRIUMF Injector for the e-Linac Project", in *Proc. LINAC'10*, Tsukuba, Japan, September 2010, paper TH202. [Online]. Available: http://jacow.org/LINAC2010/papers/th202.pdf

[9] R. Baartman, "Energy deposition and Temperature Time Constants", TRIUMF, Tech. Rep. TRI-BN-14-07, 2014.